

Long-period grating based coupler for multi-core fiber systems

Liliana M. Sousa, *Student Member, IEEE, Student Member, OSA*, Joana Vieira, Margarida Facão, Gil M. Fernandes, Rogério Nogueira, *Member, IEEE, Senior, Member, OSA*, and Ana M. Rocha, *Member, OSA*

Abstract—In this work, we propose and demonstrate numerically a long-period grating (LPG) based technique to couple light from a single-mode fiber (SMF) to all cores of a multi-core fiber (MCF), i.e., an SMF to MCF coupler. The light launched into the SMF core is coupled to the SMF cladding due to the LPG inscribed in the core. Then, the optical power is transferred between fibers claddings, enhanced by the reduction of the SMF cladding radius. Finally, the MCF cladding optical power is distributed by all cores of the MCF due to identical LPGs inscribed in them. We use the coupled-mode theory to study and design the proposed device. We achieve a coupling efficiency of approximately 90% of the input power in a total length of 15.1 cm. We also study the coupler's sensitivity to the SMF radius and LPGs period. Results show that the proposed device can improve the pumping efficiency of MCF amplifiers.

Index Terms—Fiber gratings, Optical amplifiers, Optical fiber devices

I. INTRODUCTION

The exponential growth of the data demand has led to an imminent optical networks exhaustion [1], [2]. Space Division Multiplexing (SDM) has the potential to be an efficient and, therefore, sustainable approach to solve it. SDM has been pointed out as a way to overcome the limit of the capacity of the standard single-mode fiber (SMF) as it adds new pathways to deliver even more data [2], [3]. It can be implemented using multi-core fibers (MCFs), few-mode fibers or the combination of both [2], [3]. Large capacity over long-distance transmission is simpler to achieve by using the weakly-coupled single-mode MCFs [2], [4]. The single-mode propagation is stable and the additional cores directly increase the total fiber capacity [2]. Therefore, these fibers can support high spectral-efficient modulation formats without the need of high-order multiple-input multiple-output (MIMO) digital signal processing [4].

However, SDM implementation depends on the availability of several compatible devices, such as optical amplifiers and multi-core (MC) couplers [2], [4]. If these new devices are

based on component sharing, they will contribute to reduce the number of components, the overall cost and the power consumption of the transmission system [1], [5]. Therefore, SDM will contribute not only to increase the capacity of the current systems, but also to develop more efficient and affordable optical networks. Thus, it is mandatory to develop component sharing based devices, such as MC optical amplifiers that are able to amplify all the channels by sharing a single pump source. One approach already proposed is a cladding pumping scheme, in which all the cores are simultaneously pumped by the light launched into the cladding of an MC double-clad fiber [2], [6]. However, this approach faces some issues, for example, the small overlap between the cores and the cladding fields that reduces the efficiency [7]. In fact, it was estimated that the MCF cores couple just 15% of the power launched in the MCF cladding [6]. Another approach to pump sharing uses free space optics [2], [5], whose alignment sensitivity may compromise its commercial viability.

The coupling between two SMFs promoted by long-period gratings (LPG) inscribed in their cores was already experimentally demonstrated [8], [9]. A high coupling efficiency is achieved by using an index-matching gel [9]. In [9], etching the cladding of the fibers was also suggested to improve the coupling. Concerning MCFs, power transfer between the two cores of a twin core fiber was experimentally achieved with LPGs [10], [11]. Furthermore, an LPG based scheme to distribute a single pump launched in one core of an MCF to all the other ones was also demonstrated with promising results [12], [13]. However, this technique relies on splicing the MCF and a fan-in fan-out to launch light into each core. In order to solve this, an LPG based SMF to MCF coupler was already proposed [14], but issues regarding the coupler efficiency arose, due to the periodic nature of the LPGs.

Here, we propose an improved LPG based SMF to MCF coupler by introducing an offset distance between the SMF and the MCF LPGs, with which we estimate that 90% of the input power launched in the SMF core will be distributed by all the MCF cores. For that purpose, we numerically analyze the coupling between an SMF to an MCF in terms of power transfer. For this, we first search for the coupler parameters that maximize the power transfer, and then we study the mode power evolution along the designed coupler. We also analyze the coupler sensitivity to those parameters and its wavelength selectivity. This study will support the realization of an SMF to an MCF pump coupler, that can boost the development of efficient and low cost SDM-MC amplifiers.

Manuscript received February 26, 2021. This work was funded by FCT-Fundação para a Ciência e Tecnologia through European Regional Development Fund (FEDER), and the Competitiveness and Internationalization Operational Programme (COMPETE 2020) of the Portugal 2020 framework and national funds under the projects MCTechs (POCI-01-0145-FEDER-029282), UIDB/50008/2020-UIDP/50008/2020, Liliana Sousa PhD grant POCH Program SFRH/BD/144226/2019 and Ana M. Rocha contract program 1337.

L. M. Sousa, J. Vieira, G. M. Fernandes, R. Nogueira and A. M. Rocha are with Instituto de Telecomunicações and Universidade de Aveiro, Campus Universitário de Santiago, 3810-193 Aveiro, Portugal (e-mail: sousa.liliana@ua.pt; joana.saraiva.vieira@ua.pt; gfernandes@av.it.pt; rnogueira@av.it.pt; amrocha@av.it.pt).

M. Facão is with i3N and Universidade de Aveiro, Campus Universitário de Santiago, 3810-193 Aveiro, Portugal (e-mail: mfacao@ua.pt).

II. CONCEPT

LPGs are induced periodic perturbations of the optical fiber refractive index, with periods in the range of 100 μm up to 1 mm, that induce coupling between modes traveling in the same direction, at the resonant wavelength [15], [16]. Therefore LPGs promote the selective coupling between modes, in SMFs, typically between the core fundamental mode and the cladding modes. Moreover, the electromagnetic fields associated with the cladding modes are not confined within the limits of the optical fiber, but extend outside the fiber as evanescent field. If the evanescent field overlaps another fiber, the coupling between the cladding modes of both fibers may happen.

The proposed SMF to MCF coupler is based on the scheme displayed in Fig. 1. The considered device can distribute a single pump source to all the cores of a 4-core fiber. The LPGs are inscribed in all cores of the two fibers, but are longitudinally separated by a given distance. Along this offset distance, the SMF and the MCF are close and parallel to each other. Thus, the proposed coupler is divided in three sections. Section I consists of an LPG inscribed in the SMF. In this section the pump source launched in the SMF core is transferred to its cladding due to the LPG. In section II, the optical power is transferred between the claddings of both fibers through the evanescent field. In section III, the optical power in the MCF cladding is distributed among the MCF cores due to the identical LPGs inscribed in each core. Since LPGs are wavelength selective, the optical pump experiences the LPG, designed to match its wavelength, while the remaining transmitted signals traveling in the MCF cores will not be affected. We consider the SMF and the MCF arranged as displayed in Fig. 1 and immersed in an index-matching medium with a refractive index close to the cladding refractive index in order to increase the evanescent field coupling and, in this way, increase the power transfer between the fibers [9]. The SMF and MCF LPGs periods are Λ_S and Λ_M , respectively. The LPGs periods are set in order to maximize the power transfer between the fibers cores and cladding.

In this work, we considered a standard SMF with a cladding radius of 62.5 μm and a core radius of $r_S = 4.1 \mu\text{m}$. The MCF considered is a 4-core fiber identical to the commercial fiber SM-4C1500(8.0/125)/001 from Fibercore [17], i.e., with a cladding radius of 62.5 μm and a core radius of $r_M = 3.6 \mu\text{m}$. The four cores of the MCF are equally spaced from each other and have the same distance to the fiber center. The distance between the cores is $d = 50 \mu\text{m}$. The claddings material is assumed to be pure silica and the cores material is GeO_2 doped silica with a concentration of 3% and 5% for the SMF and MCF cores, respectively. The refractive indexes of the materials of the fibers are calculated using a Sellmeier equation [18]. The LPGs are assumed to have the same index modulation with an amplitude of $\delta n = 5 \times 10^{-4}$, in all cores of the two fibers. Several techniques can be used to fabricate LPGs, such as ultraviolet (UV) laser irradiation [19], CO_2 laser irradiation [20] and femtosecond laser irradiation [21]. As we are considering the UV laser irradiation technique, the optical fibers have to be previously loaded with H_2 to increase the

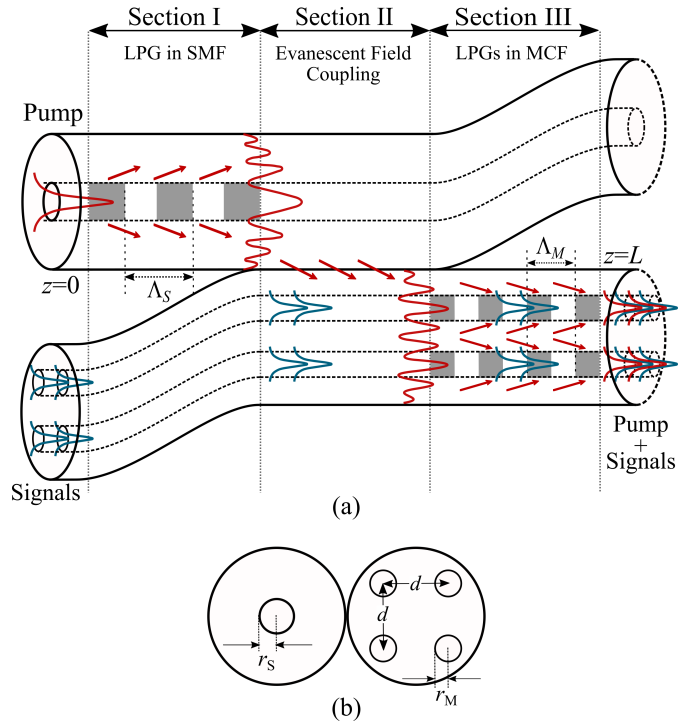


Fig. 1: Schematic diagram of the (a) proposed LPG based SMF to MCF coupler and (b) cross section of the considered fibers.

cores sensitivity to UV light and, therefore, achieve a high refractive index modulation [19].

III. THEORETICAL ANALYSIS

We use the coupled-mode theory to study the power transfer between the optical modes in the proposed device. In the presence of a dielectric perturbation, the optical modes propagating through an optical fiber can exchange power. Therefore, the evolution of the slowly varying amplitude of mode p , A_p , along z can be given by [16]:

$$\frac{dA_p}{dz} = i \sum_q A_q(z) \kappa_{qp} \exp[i(\beta_q - \beta_p)z] \quad (1)$$

where A_q is the slowly varying amplitude of mode q , β_q and β_p are the propagation constants of the mode q and p , respectively, and κ_{qp} is the transverse coupling coefficient between modes q and p . κ_{qp} is given by [16]:

$$\kappa_{qp} = \frac{\omega}{4} \iint_{\infty} \Delta\epsilon(x, y, z) \mathbf{E}_q \cdot \mathbf{E}_p^* dx dy \quad (2)$$

with ω being the angular frequency of the light, $\Delta\epsilon(x, y, z)$ is the perturbation to the electric permittivity and \mathbf{E}_q and \mathbf{E}_p are the normalized transverse component of the electric fields of modes q and p , respectively. We consider two types of coupling coefficients (K_{qp} and C_{qp}), depending on the $\Delta\epsilon$ nature. K_{qp} is due to the LPGs, being considered in section I and III, and C_{qp} is due to the evanescent field coupling, being only considered in section II of the coupler (see Fig. 1).

We assume that the LPG inscription introduces, along z , a refractive index modulation in the core. Therefore, K_{qp} is given by [12]:

$$K_{qp} = \sigma_{qp} \left[1 + \cos \left(\frac{2\pi}{\Lambda} z \right) \right] \quad (3)$$

where

$$\sigma_{qp} = \frac{\omega \epsilon_0 n_c \delta n}{2} \iint_{\text{core}} \mathbf{E}_q \cdot \mathbf{E}_p^* dx dy \quad (4)$$

being ϵ_0 the vacuum permittivity, Λ the LPG period, n_c the core refractive index and δn the index modulation amplitude. In that case, we can choose the resonant wavelength, λ_{\max} , by setting Λ according to [16]:

$$\frac{1}{\lambda_{\max}} = \left(\frac{\sigma_{\text{clcl}} - \sigma_{\text{cc}}}{2\pi} + \frac{1}{\Lambda} \right) / (n_{\text{eff}_c} - n_{\text{eff}_{\text{cl}}}) \quad (5)$$

with n_{eff_c} and $n_{\text{eff}_{\text{cl}}}$ being the effective refractive indexes of the core fundamental mode and cladding mode, respectively, and σ_{cc} and σ_{clcl} being the self-coupling coefficients for the same modes.

Considering the coupling between cladding modes of different fibers by evanescent field, the coupling coefficient is given by [22], [23]:

$$C_{qp} = \frac{\omega \epsilon_0}{4} \int_{-\infty}^{+\infty} \int_{-\infty}^{+\infty} (N^2 - N_q^2) \mathbf{E}_q \cdot \mathbf{E}_p^* dx dy \quad (6)$$

being N^2 the refractive index distribution of the two fibers. If mode q is traveling along the SMF, $N^2 - N_q^2$ is $n_{\text{cl}}^2 - n_e^2$ in the MCF region, with n_{cl} and n_e as the refractive index of the cladding and index-matching gel, respectively. In all the other regions, $N^2 - N_q^2$ is zero. In the same way, if mode q is in the MCF, $N^2 - N_q^2$ is $n_{\text{cl}}^2 - n_e^2$ in the SMF region and zero in the remaining regions. Thus, for modes self-coupling (when $p = q$), the overlap integral is calculated using the cladding of the other fiber, since it is the presence of the MCF that imposes a dielectric perturbation on the propagation of the SMF modes and vice versa. We do not consider the cores contribution in the evanescent field coupling, as it is negligible in their region.

For two similar waveguides, the maximum fraction of power that can be transferred between them is found by integrating (1), considering one optical mode for each waveguide and setting $\kappa_{qp} = C_{qp}$. In this case, there is an analytical solution to calculate the maximum fraction of power transferred, which is [22]:

$$P_t = \frac{|C_{qp}|^2}{|C_{qp}|^2 + \delta^2} \quad (7)$$

where $2\delta = (\beta_q + C_{qq}) - (\beta_p + C_{pp})$. Total power transfer should happen when $\delta = 0$, i.e., when the effective refractive indexes of the optical modes are similar. When two waveguides are equal, like two SMFs with the same characteristics, the effective refractive indexes of the optical modes are always equal. If the waveguides are different from each other, as the SMF and MCF that we are considering, we have to choose modes with similar effective refractive indexes to maximize the power transfer. Then, the length of section II is set accordingly to the coupling distance, i.e., the distance needed to achieve

the maximum power transfer between fibers, which is given by [22]:

$$d_c = \frac{\pi}{2\sqrt{|C_{qp}|^2 + \delta^2}}. \quad (8)$$

In order to achieve the maximum coupling between the fibers, we had to take into account two factors in the cladding modes choice. In LPGs with azimuthal symmetric index changes, like the ones we are considering, the coupling between the core and cladding modes just occurs if they present the same azimuthal symmetry [16]. So we need to use cladding modes that present the same azimuthal symmetry as the core fundamental mode. And, we need to choose a pair of modes, one from each fiber, that maximizes the coupling between the two fibers.

IV. RESULTS

To obtain the electric field distribution (\mathbf{E}) and the effective refractive index (n_{eff}) of each optical mode for both fibers, we used the Wave Optics module of the software package Comsol Multiphysics[®] that solves the vectorial Helmholtz equation. For this calculation, we assumed the bare fibers surrounded by an index-matching gel with a refractive index of 1.4386. This value was estimated from the experimental curve of the Thorlabs G608N3 index-matching gel, at 1480 nm. We considered this wavelength, since it is the one used as pump light in Raman amplification. Then, we used a Runge Kutta method to integrate the coupled mode equations system (1) in order to obtain the modes power evolution in the SMF and MCF along z .

A. Power transfer between fibers

We started by studying the coupling between the cladding modes of the fibers (section II). We considered ten azimuthally symmetric cladding modes for the SMF and thirteen for the MCF. For each SMF-MCF cladding mode pair, we calculated the maximum power transfer from the SMF to the MCF cladding mode using (7) and the coupling distance using (8). We intend to maximize the power coupling in a short coupling distance. We achieved a maximum power transfer of $P_t \approx 40\%$ from the SMF to the MCF cladding, with a coupling distance of $d_c \approx 2$ cm, for a pair of modes with similar effective refractive indexes, 1.440724 for the SMF (the optical mode $\text{HE}_{1,10}$) and 1.440752 for the MCF. However, in order to reach high efficiency on the proposed coupler, we need higher power transfer between the claddings.

Reducing the cladding radius may lead to a higher similarity, in terms of the propagation constants, between modes of different fibers and also enhance the evanescent field of the cladding modes [9], which may increase the coupling between fibers and decrease the coupling distance. Experimentally, this reduction can be achieved by chemical attack of the fiber [24]. We have considered only the reduction of the cladding of the SMF, because the SMF core is farther from the exterior than the cores in the MCF, which makes its mode less affected by the cladding reduction.

As may be seen in Fig. 2, the change in the effective refractive index with the SMF radius is smoother for higher

radius and lower-order optical modes. Thus, to decrease the sensibility of the coupler to the SMF radius, we focused on the lower-order modes. Furthermore, using these modes will improve the selectivity of the coupling since lower-order modes have higher difference between the propagation constants. For each SMF radius and SMF-MCF cladding modes pair, we calculated P_t and d_c , searching for an SMF radius and a pair of modes that yield high power transfer over a short distance.

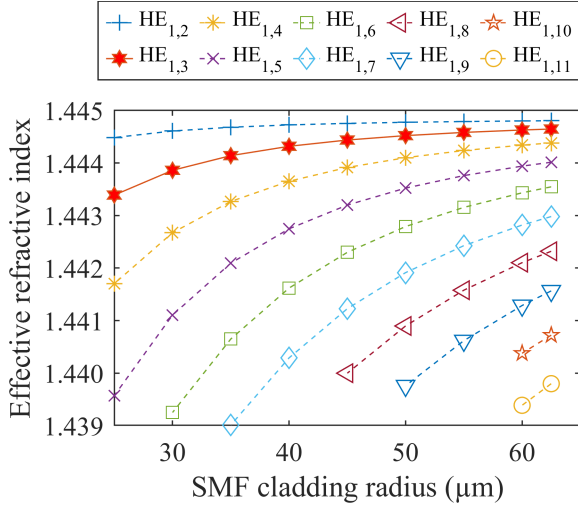


Fig. 2: Effective refractive index of the SMF cladding modes as a function of its radius. The solid line corresponds to the SMF mode chosen.

For an SMF cladding radius of $r_{\text{SMF}} = 46 \mu\text{m}$, we found a pair of modes that fulfills these requirements, yielding a power transfer of $\sim 73\%$ in a coupling distance of 8 cm. Then, we calculated the modes power evolution in section II by integrating (1) considering the power launched into the selected SMF cladding mode (i.e., half of the power into one of its polarization state and the other half into the other state) and no LPG inscription, for different SMF cladding radii around $r_{\text{SMF}} = 46 \mu\text{m}$. This analysis was closer to the actual situation by considering the adjacent MCF and SMF modes, i.e., the cladding modes right above/below the selected cladding modes. We found that considering eight MCF and four SMF cladding modes is sufficient, since adding more cladding modes did not affect the calculations significantly (less than 1% difference in the power transfer) for $r_{\text{SMF}} = 46 \mu\text{m}$. The pair of the selected cladding modes and the number of considered adjacent cladding modes was maintained for other SMF cladding radii. For each considered mode, its two orthogonal polarization states were used in the calculations. Figure 3 displays the maximum power transferred from the selected SMF cladding mode to the selected MCF cladding mode and the coupling distance needed. A maximum power transfer of 96% between the chosen cladding modes occurs for a radius of $r_{\text{SMF}} = 46.3 \mu\text{m}$ and a coupling distance of 9.8 cm. The electric field distributions of these modes are shown in Fig. 4.

With this approach, we obtained feasible results for the SMF to MCF coupler, so we proceeded with the study of

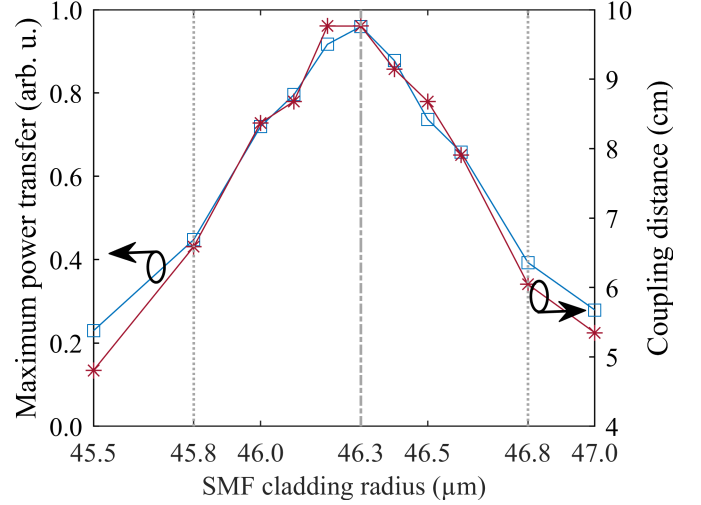


Fig. 3: Power transfer between the selected cladding modes (blue) and the coupling distance (red) for SMF cladding radii around $46 \mu\text{m}$.

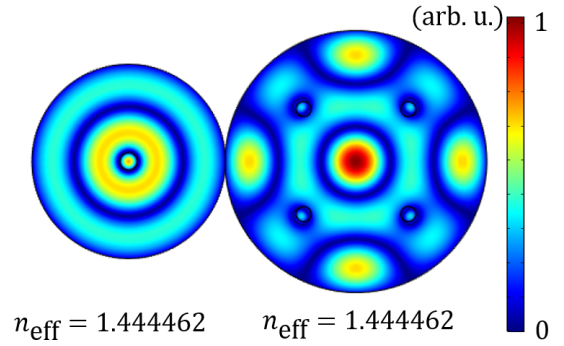


Fig. 4: Normalized electric field distribution of the cladding modes chosen, at a wavelength of 1480 nm, in the SMF ($\text{HE}_{1,3}$) with a cladding radius of $46.3 \mu\text{m}$ (left) and the MCF (right).

the proposed device.

B. Single-mode fiber to multi-core fiber coupler

We expect that the etching process will produce a final SMF radius whose experimental error will be less than $0.5 \mu\text{m}$ [24]. To take into account this error, we calculated the modes power evolution along the proposed SMF to MCF coupler for three cases, the best scenario found ($r_{\text{SMF}} = 46.3 \mu\text{m}$) and the ones for which the SMF cladding radius was $0.5 \mu\text{m}$ below and above the selected SMF cladding radius ($45.8 \mu\text{m}$ and $46.8 \mu\text{m}$). In this way, we have integrated the equations system (1) considering one mode for each core, one selected mode for each cladding and the adjacent cladding modes. To promote the total power transfer between the core and chosen cladding modes (displayed in Fig. 4), we calculated the LPGs period using (5) for the SMF with the selected reduced radius and for the MCF, considering a resonant wavelength of 1480 nm. As the effective refractive indexes of the core modes are 1.446702

(SMF) and 1.448527 (MCF), we set the LPG periods as $\Lambda_S = 569 \mu\text{m}$ and $\Lambda_M = 332 \mu\text{m}$. Experimentally, we intend to inscribe the SMF LPG before the etching process to monitor the LPG spectrum during this process. Therefore, we used the same Λ_S for all the situations considered.

Figure 5 displays the modes power evolution for the three cases. The light launched in the SMF core is transferred to its cladding, which is promoted by the LPG inscribed on the SMF core. For the best case scenario, the optical power of the selected SMF cladding mode achieves its maximum at $34 \Lambda_S$ ($\sim 1.9 \text{ cm}$). Along section II, the light from the SMF cladding mode is transferred to the MCF cladding modes by evanescent field. Most of the light is transferred to the selected MCF cladding mode ($\sim -0.19 \text{ dB}$), however a small part is coupled to the adjacent cladding modes. Section II ends when the power of the selected MCF cladding mode achieves its maximum, at 9.8 cm of length. Note that, as displayed in Fig. 5, the end of section II does not coincide with the minimum power of the selected SMF cladding mode due to the interaction with the adjacent cladding modes. In section III, the SMF and MCF are separated, ending the evanescent field interaction, and the SMF cladding mode power stays in the SMF. The power of the selected MCF cladding mode is distributed by all the MCF cores due the LPGs inscribed in each MCF core. We are assuming that the LPGs are identical, making the power in the MCF cores increase at a similar rate, which leads to an even distribution of power among them. The length of the MCF LPGs is set to $103 \Lambda_M$ ($\sim 3.4 \text{ cm}$), which corresponds to the maximum power in the MCF cores. A mean power transfer to each MCF core of about -6.5 dB ($\sim 22.6\%$ of the input power) was achieved, which corresponds to a total power transfer from the SMF to the MCF cores of -0.5 dB ($\sim 90\%$ of the input power). The coupler length is given by the sum of the length of the three sections, being around 15.1 cm .

In the studied cases that deviate from the selected SMF cladding radius, the SMF LPG period and length will not be optimal for the considered modes. Thus, the fraction of power transferred to the SMF cladding reduces to 96% and 93% of the input power, for $r_{\text{SMF}} = 46.8 \mu\text{m}$ and $r_{\text{SMF}} = 45.8 \mu\text{m}$, respectively. As may be seen in Fig. 5, section II length was updated in each case to maximize the power transfer to the MCF cladding (6.0 cm and 6.2 cm when $r_{\text{SMF}} = 46.8 \mu\text{m}$ and $r_{\text{SMF}} = 45.8 \mu\text{m}$, respectively). In both cases, we achieved a mean power of about -10.5 dB ($\sim 9\%$ of the input power) per core, which corresponds to a total output of -4.4 dB ($\sim 36\%$ of the input power). In that case, the coupler length is $\sim 11.4 \text{ cm}$ and 11.6 cm for $r_{\text{SMF}} = 46.8 \mu\text{m}$ and $r_{\text{SMF}} = 45.8 \mu\text{m}$, respectively.

Besides the SMF radius, the experimental LPG period may slightly differ from the defined value. Thus, we also studied how a small variation in the LPG period will affect the power transfer in the coupler. We considered this variation to be in steps of $0.5 \mu\text{m}$, because the error of the LPG inscription will be less than $0.5 \mu\text{m}$ if precision stages with resolution of $0.1 \mu\text{m}$ are used. We maintained the length of section I and III as $34 \Lambda_S$ and $103 \Lambda_M$, respectively. We also maintained the offset distance (section II length) as 9.8 cm . Figure 6 displays the total power transfer, normalized by the SMF input power,

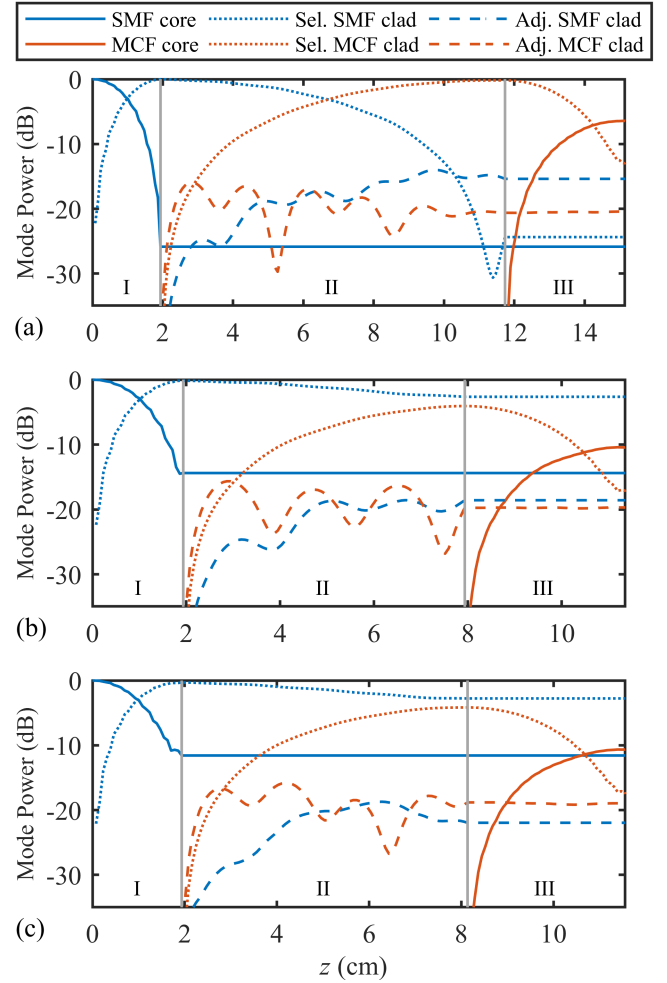


Fig. 5: Mode power evolution along the coupler for an SMF cladding radius of (a) $46.3 \mu\text{m}$, (b) $46.8 \mu\text{m}$ and (c) $45.8 \mu\text{m}$. Sel. and Adj. correspond to the selected cladding mode and to the sum of the considered adjacent cladding modes, respectively. The power in each MCF core presents a similar evolution as the one displayed. The coupler's sections I, II and III are displayed in the corresponding regions.

from the SMF to the MCF (sum of the normalized output power of each MCF core) as a function of the SMF and MCF LPG periods. The power transfer sensitivity to the SMF LPG period is low, the fraction of output power is over 40% of the input power within the range of SMF LPG periods of $562 \mu\text{m}$ to $575 \mu\text{m}$. However, the power transfer is more sensitive to the MCF LPG period, it should be in a $3 \mu\text{m}$ range to yield an output power higher than 40% . Nevertheless, LPGs can be inscribed with a period error less than $1 \mu\text{m}$ [25]. This can also indicate that this type of coupler may be temperature sensitive, not only due to the thermal expansion of silica glass but also to its thermo-optic behaviour. Thus, this coupler should be under temperature control. However, temperature can be additionally employed to fine tune the LPG, if needed.

The index modulation amplitude, δn , can also slightly differ from the defined one. However, in this case, the length of the LPG may be updated accordingly, to maintain the same

transmission level [16].

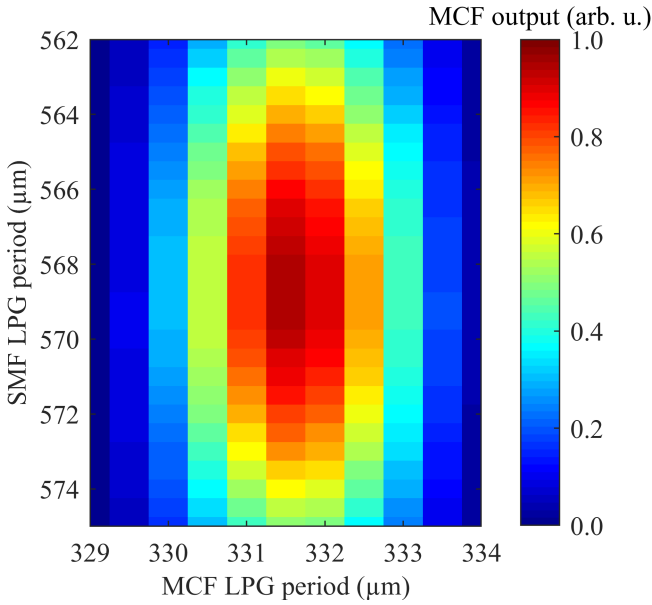


Fig. 6: Normalized MCF total output as a function of SMF and MCF LPGs periods for an SMF cladding radius of $46.3 \mu\text{m}$. A step of $0.5 \mu\text{m}$ was considered for the LPGs period.

To obtain the transmission spectrum and confirm the wavelength selectivity, we calculated the evolution of the modes power along the coupler for the best case scenario and wavelengths in the range from 1460 nm to 1565 nm . We obtained the transmission spectrum, displayed in Fig. 7, using the mode power at the end of the coupler for the different wavelengths. We observe an attenuation band in the SMF core and a transmission band in the MCF cores, around the wavelength of 1480 nm . The transmission band presents spectral sidelobes, which are expected in the spectrum of a periodic optical resonance structure such as LPGs [16]. However, the transmission of these sidelobes in the C band is very low, less than -40 dB . Thus, the optical signals, travelling in the MCF, will not be affected by them.

The proposed approach can be applied, with similar results, in MCFs with ring geometry. This approach can also be applied in other geometries, however, in the design of the LPGs of the MCF, we should also take into account the differences in the coupling coefficients between the cladding mode and cores modes. By adjusting the proper parameters, the proposed scheme should be able to distribute light at other wavelengths, e.g., pump light at 980 nm , for erbium-doped fiber amplification.

V. CONCLUSION

The optical power transfer from an SMF to all cores of an MCF was numerically demonstrated. The considered device is able to distribute a single pump source injected in an SMF core to all the cores of a 4-core fiber. A maximum power transfer of approximately 90% (-0.6 dB), an average of $\sim 22.6\%$ (-6.5 dB) per MCF core was achieved, using LPGs with 1.9 cm (SMF core) and 3.4 cm (MCF cores) of length,

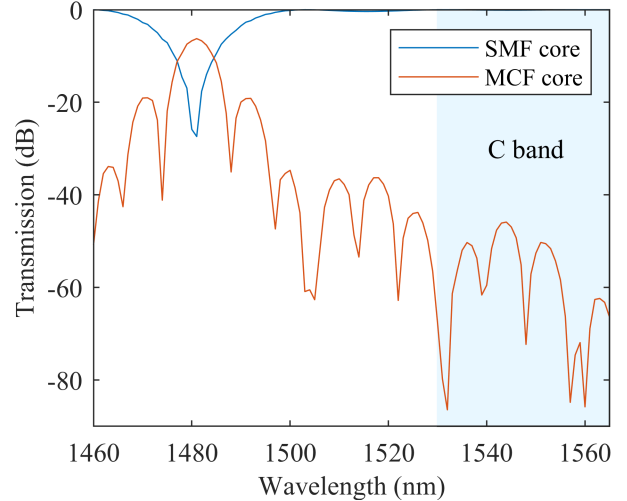


Fig. 7: Transmission spectrum of the coupler when optical power is launched into the SMF core. Each MCF core presents a similar behaviour as the one displayed.

and an offset distance of 9.8 cm , leading to a device with a total length of $\sim 15.1 \text{ cm}$. We studied the sensitivity of the coupler to the SMF cladding radius by considering an SMF radius below and above the selected one, achieving a power transfer in the worst case of 36% . The coupler sensitivity to the LPGs period was also analyzed, being possible to still couple 40% of the input power to the MCF for SMF and MCF periods ranging from $562 \mu\text{m}$ to $575 \mu\text{m}$ and from $330.5 \mu\text{m}$ to $333 \mu\text{m}$, respectively. The coupling efficiency of the proposed coupler may increase the energy efficiency of the overall amplification subsystem, resulting therefore in an enhanced in-line pumping scheme for MCF amplifiers. We also demonstrated the selective nature of the coupler, which promotes the optical power transfer at a wavelength around 1480 nm . Although further optimization has to be done, this numerical analysis shows that this technique can be used to produce SMF to MCF couplers for MCFs transmission systems.

REFERENCES

- [1] D. J. Richardson, J. M. Nelson, and E. Lynn, "Space-division multiplexing in optical fibres," *Nature Photonics*, vol. 7, no. 5, pp. 354–362, April 2013.
- [2] Y. Awaji, "Review of space-division multiplexing technologies in optical communications," *IEICE Transactions on Communications*, vol. 102, no. 1, pp. 1–16, 2019.
- [3] T. Matsui, Y. Sagae, T. Sakamoto, and K. Nakajima, "Design and applicability of multi-core fibers with standard cladding diameter," *Journal of Lightwave Technology*, vol. 38, no. 21, pp. 6065–6070, 2020.
- [4] K. Saitoh and S. Matsuo, "Multicore fiber technology," *Journal of Lightwave Technology*, vol. 34, no. 1, pp. 55–66, 2016.
- [5] J. Sakaguchi, W. Klaus, B. J. Puttnam, J. M. D. Mendinueta, Y. Awaji, and N. Wada, "Progress of space division multiplexing technology for future optical networks," in *2014 12th International Conference on Optical Internet 2014 (COIN)*. IEEE, 2014, pp. 1–2.
- [6] K. S. Abedin, J. M. Fini, T. F. Thierry, B. Zhu, M. F. Yan, L. Bansal, F. V. Dimarcello, E. M. Monberg, and D. J. DiGiovanni, "Seven-core erbium-doped double-clad fiber amplifier pumped simultaneously by side-coupled multimode fiber," *Optics Letters*, vol. 39, no. 4, pp. 993–996, 2014.

- [7] H. Ono, K. Takenaga, K. Ichii, and M. Yamada, "Amplification technology for multi-core fiber transmission," in *2014 IEEE Photonics Society Summer Topical Meeting Series*. IEEE, 2014, pp. 146–147.
- [8] Y. Liu, K. S. Chiang, Y. J. Rao, Z. L. Ran, and T. Zhu, "Light coupling between two parallel co2-laser written long-period fiber gratings," *Optics Express*, vol. 15, no. 26, pp. 17 645–17 651, 2007.
- [9] K. S. Chiang, Y. Liu, M. N. Ng, and S. Li, "Coupling between two parallel long-period fibre gratings," *Electronics Letters*, vol. 36, no. 16, pp. 1408–1409, 2000.
- [10] X. Xu, X. Ouyang, A. Zhou, H. Deng, and L. Yuan, "An integrated wavelength selective coupler based on long period grating written in twin-core fiber," *Optics Communications*, vol. 445, pp. 1–4, 2019.
- [11] M. Wang, C. Guan, Z. Yu, J. Yang, Z. Zhu, J. Shi, J. Yang, and L. Yuan, "Core-independent inscription of lpgs in twin-core fiber by co2 laser and coupling between lpgs," *Optics express*, vol. 27, no. 11, pp. 15 786–15 793, 2019.
- [12] A. M. Rocha, T. Almeida, R. N. Nogueira, and M. Facão, "Analysis of power transfer on multicore fibers with long-period gratings," *Optics letters*, vol. 40, no. 2, pp. 292–295, 2015.
- [13] T. Almeida, A. Shahpari, A. Rocha, R. Oliveira, F. Guiomar, A. Pinto, A. Teixeira, P. André, and R. Nogueira, "Experimental demonstration of selective core coupling in multicore fibers of a 200 gb/s dp-16qam signal," in *Optical Fiber Communication Conference*. Optical Society of America, 2016, pp. Tu3I–4.
- [14] L. M. Sousa, M. Facão, G. M. Fernandes, R. N. Nogueira, and A. M. Rocha, "Long-period grating based single-mode fiber to multi-core fiber pump coupler," in *Frontiers in Optics*. Optical Society of America, 2020, pp. FTh2E–3.
- [15] K. S. Chiang and Q. Liu, "Long-period grating devices for application in optical communication," in *Proceedings of the 5th International Conference on Optical Communications and Networks (ICOON 2006)*, 2006, pp. 128–133.
- [16] T. Erdogan, "Fiber grating spectra," *Journal of lightwave technology*, vol. 15, no. 8, pp. 1277–1294, 1997.
- [17] FIBERCORE. Multicore Fiber [Online]. Available: <https://fibercore.humaneticsgroup.com/products/multicore-fiber/multicore-fiber/sm-4c150080125001>.
- [18] J. W. Fleming, "Dispersion in geo 2-sio 2 glasses," *Applied Optics*, vol. 23, no. 24, pp. 4486–4493, 1984.
- [19] A. M. Vengsarkar, P. J. Lemaire, J. B. Judkins, V. Bhatia, T. Erdogan, and J. E. Sipe, "Long-period fiber gratings as band-rejection filters," *Journal of lightwave technology*, vol. 14, no. 1, pp. 58–65, 1996.
- [20] T. Almeida, R. Oliveira, P. André, A. Rocha, M. Facão, and R. Nogueira, "Automated technique to inscribe reproducible long-period gratings using a co2 laser splicer," *Optics letters*, vol. 42, no. 10, pp. 1994–1997, 2017.
- [21] M. Heck, R. G. Krämer, T. Ullsperger, T. A. Goebel, D. Richter, A. Tünnermann, and S. Nolte, "Efficient long period fiber gratings inscribed with femtosecond pulses and an amplitude mask," *Optics letters*, vol. 44, no. 16, pp. 3980–3983, 2019.
- [22] A. Yariv and P. Yeh, *Photonics: optical electronics in modern communications*, 6th ed. Oxford Univ., 2006, pp. 611–615.
- [23] K. Okamoto, *Fundamentals of optical waveguides*, 2nd ed. Academic press, 2006.
- [24] J. F. Kuhne, A. M. Rocha, V. de Oliveira, H. J. Kalinowski, and R. C. Kamikawachi, "Experimental and numerical study on refractive index sensors based on fibre bragg gratings inscribed in multimode fibre," *Measurement Science and Technology*, vol. 29, no. 2, p. 025102, 2018.
- [25] L. Everall, R. Fallon, J. Williams, L. Zhang, and I. Bennion, "Flexible fabrication of long-period in-fiber gratings," in *Technical Digest. Summaries of Papers Presented at the Conference on Lasers and Electro-Optics. Conference Edition. 1998 Technical Digest Series, Vol. 6 (IEEE Cat. No. 98CH36178)*. IEEE, 1998, pp. 513–514.